PHYSICAL REVIEW B **80**, 241407(R) (2009)

Three-fold diffraction symmetry in epitaxial graphene and the SiC substrate

D. A. Siegel,[1,2] S. Y. Zhou,[1,2] F. El Gabaly,[3] A. K. Schmid,[2] K. F. McCarty,[3] and A. Lanzara[1,2,*]
[1]*Department of Physics, University of California, Berkeley, California 94720, USA*
[2]*Materials Sciences Division, Lawrence Berkeley National Laboratory, Berkeley, California 94720, USA*
[3]*Sandia National Laboratories, Livermore, California 94551, USA*
(Received 8 October 2009; published 10 December 2009)

The crystallographic symmetries and spatial distribution of stacking domains in graphene films on 6H-SiC(0001) have been studied by low-energy electron diffraction and dark-field imaging in a low-energy electron microscope. We find that the graphene diffraction spots from two and three atomic layers of graphene have three-fold symmetry consistent with *AB* (Bernal or rhombohedral) stacking of the layers. On the contrary, graphene diffraction spots from the buffer layer and monolayer graphene have apparent six-fold symmetry, although the three-fold nature of the satellite spots indicates a more complex periodicity in the graphene sheets.

DOI: 10.1103/PhysRevB.80.241407 PACS number(s): 61.48.De, 68.65.−k, 61.05.jh, 68.37.Nq

The past few years have witnessed a growing need to identify new methods for the synthesis of graphene films for both basic research and industrial applications. Of all the methods explored so far, substrate growth methods seem the most promising due to the ease and reliability of growth of large-scale films.[1–3] However, the presence of a substrate can often impose nonbulklike structures on overlayer films that alter their properties; one well-known example is the case of thin magnetic films.[4] In graphene, the choice of substrate can have a major impact on the properties of the film as well. For example, substrates that break the *A*-*B* sublattice symmetry (or equivalently the six-fold rotational symmetry) of graphene, such as hexagonal boron nitride or *AB*-stacked bilayer graphene, result in the opening of a band gap and the destruction of the Dirac behavior of the quasiparticles in graphene.[5–10] On the other hand, substrates where this symmetry is preserved, such as graphene grown on the C face of SiC (which possesses azimuthal rotations between layers) can retain this Dirac behavior even for multilayer films.[3,11–13]

Therefore, understanding how graphene grows on top of a substrate is fundamental to engineering new graphene sheets with controlled properties. Here we will focus on epitaxial graphene grown on SiC(0001), one of the most studied graphene systems because of its potential for industrial application due to the presence of a band gap in measured as well as calculated spectra.[9,10] The mechanism behind this gap opening is still under debate, so understanding the precise structure of the graphene/buffer layer system remains an important issue.[14,15]

One way to answer questions about the structure of epitaxial graphene might be through low-energy electron diffraction (LEED), which is a more direct probe of the crystal symmetry than scanning tunneling microscope[14–16] provided that the diffraction can be performed with a spatial resolution that is smaller than the structural domains of the crystal. For example, LEED from a single Ru(0001) terrace has the three-fold symmetry of the hcp layer stacking, while LEED from a region containing multiple terraces has an averaged six-fold symmetry.[17] Similar measurements can be performed with greater spatial resolution by using dark-field low-energy electron microscopy (LEEM) imaging. Dark-field LEEM images are real-space images derived from higher order diffraction spots. This differs from bright-field LEEM, where the images are obtained from the specularly reflected beam, the (0,0) diffraction spot. Thus, dark-field LEEM can be viewed as a tool comparable to LEED, where the dark-field LEEM image is a map of the intensity of a single LEED spot as a function of sample position. Combining several such images obtained on inequivalent diffraction spots, one can determine direct evidence of asymmetries in the LEED diffraction peaks as a function of position in the LEEM image.

Here we characterize the crystallographic structure of graphene/SiC films and the spatial distribution of stacking domains by high-resolution dark-field LEEM imaging. We find that the six-fold symmetry is broken for the 1×1 SiC LEED spots, and for the 1×1 graphite LEED spots of multilayer (≥2 graphene layers in addition to the buffer layer) graphene. On the contrary, the apparent six-fold symmetry of the graphite LEED spots is preserved in the buffer layer and single-layer graphene, showing that the stacking between these two layers differs from that of bilayer graphene. Interestingly, we also observe that the 6×6 satellite spots possess three-fold symmetry for every measured film thickness. These measurements of diffraction symmetry help us to understand the properties of epitaxial graphene films.

Two atomically thin graphene samples of different thicknesses have been epitaxially grown on 6H-SiC(0001) by thermal decomposition in UHV.[18] The first graphitic layer that forms is a carbon-rich "buffer layer,"[19] which has the same σ bands as graphene but the conical dispersion of the graphene π bands is absent.[12,20] The second graphitic layer is single-layer graphene, with a band gap at the Dirac point due to the graphene substrate interaction.[9] LEEM measurements were performed at the National Center for Electron Microscopy at the Lawrence Berkeley National Laboratory to monitor and characterize the *in situ* growth.[21–23] Bright-field images show that sample 1 is mostly buffer layer with monolayer graphene present and that sample 2 is two monolayers of graphene on average, with single- and triple-layer graphene present as well. To study the crystallographic structure of these samples, dark-field LEEM and LEED were performed at Sandia National Laboratory at room temperature after transfer in air and outgassing to 1000C.

Figure 1(a) shows a typical LEED pattern[24] with single-

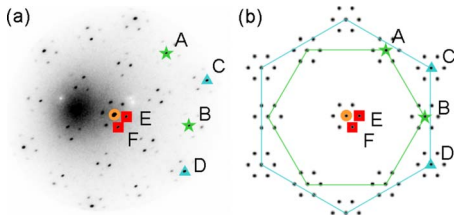

FIG. 1. (Color online) (a) A LEED image (43 eV) of an epitaxially grown graphene sample. The region of intensity to the left of center is due to secondary electrons. (b) A cartoon of the LEED image in (a) that shows the relevant sets of diffraction spots more clearly. In both panels, two SiC spots are marked with stars, two graphite spots are marked with triangles, two 6×6 spots are marked with squares, and the (0,0) spot is marked with a circle.

layer graphene and buffer layer exposed. Due to the mismatch between the graphene and the SiC lattices, there is a $(6\sqrt{(3)}\times6\sqrt{(3)})R30°$ unit cell. This unit cell appears in the diffraction pattern as bright 6×6 satellite spots around the specular beam and the first-order diffraction spots that correspond to the graphite and SiC lattice periodicities.

Figure 2 shows dark-field LEEM images from SiC LEED spots. The bright-field image, obtained from the (0,0) diffraction spot (central orange circle in Fig. 1), is shown in Fig. 2(a) and provides an accurate determination of the sample thickness by monitoring the intensity contrast as a function of electron energy (Refs. 21–23). The dark-field images from two SiC LEED spots (spots "A" and "B" in Fig. 1) are shown in Figs. 2(b) and 2(c). The direct comparison between the two dark-field images clearly shows that there are regions of the sample where the intensity is *reversed* from one LEED spot to the next (compare, e.g., the regions outlined in panels b and c). Such intensity change is more obvious when plotting the intensity difference [Fig. 2(d)] as an "asymmetry

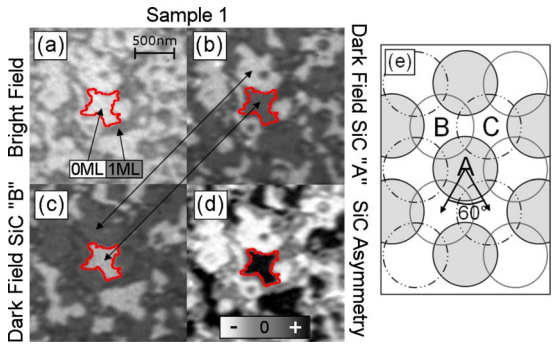

FIG. 2. (Color online) 2×2 μm LEEM images, taken at the same place on sample 1. (a) A bright-field image (3.7 eV) where the buffer layer is light gray and single-layer graphene is medium gray. (b) Dark-field image (53.0 eV) for the SiC LEED spot labeled "A" in Fig. 1. (c) Dark-field image (also 53.0 eV) for the SiC LEED spot labeled "B" in Fig. 1. (d) Dark-field contrast between the two 53.0 eV SiC LEED spots shown; panel (d) is a subtraction of panel (c) from panel (b). In panel (d), positive and negative contrast are given by the black and white regions of the image, and regions of zero contrast are gray. (e) Cartoon illustrating two ways to stack one layer above another in a closest-packed configuration; *AB* stacking differs from *AC* stacking by a 60° rotation.

TABLE I. Summary of diffraction symmetries.

Type of diffraction spot	Graphene thickness			
	Buffer Layer	One-Layer	Two-Layer	Three-Layer
SiC	Three-fold			
Graphene	Six-fold	Six-fold	Three-fold	Three-fold
Satellite	Three-fold	Three-fold	Three-fold	Three-fold

contrast image," obtained by subtracting panel (b) from panel (c). This intensity contrast is a direct measure of the asymmetry between two LEED spots. Regions that look black or white in panel (d) represent the areas of larger asymmetry, while gray in panel (d) corresponds to the regions of almost zero asymmetry. This asymmetry reflects a three-fold rather than six-fold diffraction symmetry, likely due to the three-fold symmetry of the SiC surface stacking. A stepped and terraced 6H SiC(0001) surface has, on average, six-fold crystallographic symmetry, but a single atomic terrace on the SiC surface has three-fold symmetry. The symmetry relationship between adjacent terraces separated by a step can be understood by considering the stacking sequence of layers perpendicular to the surface in 6H SiC—*ABCACB*. Consider two terraces separated by a three-layer step. If one terrace has *AB* termination, the other has *AC* termination. Since the *AB* stacking is 60° rotated from *AC* stacking, the diffraction patterns from the two terraces are also 60° rotated. This is why anywhere in panel (a) that has buffer layer is either black or white in panel (d). In contrast, the intensity of diffraction from the single-layer graphene into the SiC LEED spots is significantly lower, which limits our ability to determine the symmetry; this is likely why monolayer graphene in panel (d) is gray. A summary of these results is given in Table I.

Figure 3 presents the diffraction asymmetry from the graphite spots for monolayer and multilayer graphene from two samples. The data show that the apparent six-fold symmetry is preserved only for the buffer layer and monolayer graphene, while it is clearly broken for multilayer graphene ($\geq$2 graphene layers plus buffer layer). The local film thickness is determined from the bright-field images of panels (a) and (b). In the case of buffer layer (panel c) and monolayer graphene (panel c and d) we do not observe contrast in the asymmetry image for any electron energy studied, despite the presence of a strong signal. We note that, in comparison to panel (d), there are some regions of faint contrast in panel (c), but these artifacts are at the boundaries of domains and result from imperfections in the image subtraction process. This lack of contrast indicates that monolayer graphene maintains a six-fold diffraction pattern. The lack of three-fold symmetry is surprising since one might expect the monolayer graphene to be Bernal (or rhombohedrally) stacked above the buffer layer, as predicted by theoretical calculations.[10] There is more than one possible explanation for this result. First, graphene may still be Bernal stacked above the buffer layer if the buffer layer domain size (lateral extent) is smaller than the resolution of the LEEM (approximately 10 nm). If the domains are small, the average stack-

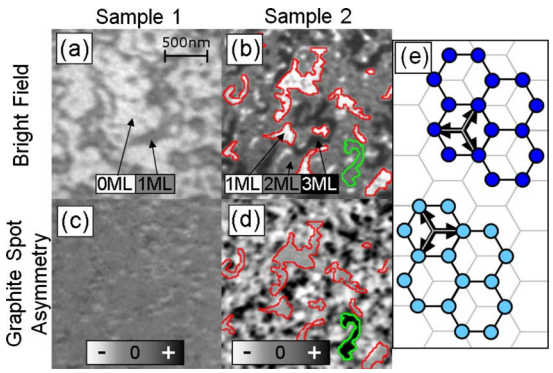

FIG. 3. (Color online) 2 μm$\times$2 μm LEEM images. (a,b) Bright-field images of two different samples. The gray scale of (a) is different from (b); (a) was taken at 3.7 eV, where the buffer layer is light gray, and single-layer graphene is medium gray. (b) was taken at 5.4 eV, where single-layer graphene is light gray or white (rippled looking), bilayer graphene is medium gray, and three-layer graphene is black. The buffer layer would be a bright white. (c,d) Dark-field contrast images from two graphite LEED spots (labeled "C" and "D" in Fig. 1), taken at 49.2 and 55.7 eV, respectively. Positive and negative contrasts are given by the black and white regions of the image, and regions of zero contrast are gray. Outlines [red (darker gray) for monolayer graphene, green (lighter gray) for bilayer] are drawn to help the comparison. (e) Cartoon that shows the two types of stacking domains in panel (d).

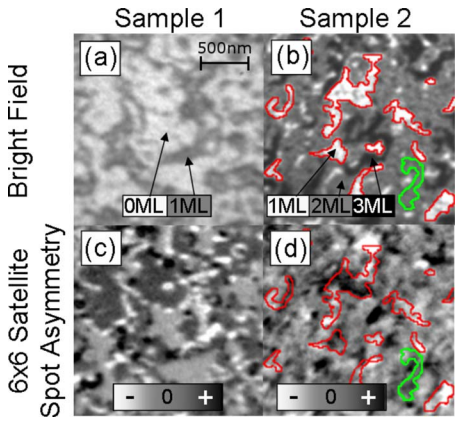

FIG. 4. (Color online) 2$\times$2 μm LEEM images. (a) and (b) Bright-field images of two samples [the same images as panels (a) and (b) of Fig. 3]. (a) was taken at 3.7 eV, where the buffer layer is light gray, and single-layer graphene is medium gray. In (b), taken at 5.4 eV, single-layer graphene is light gray or white (rippled looking), bilayer graphene is medium gray, and three-layer graphene is black. (c) and (d) Dark-field contrast of two 6$\times$6 LEED spots (labeled "E" and "F" in Fig. 1), taken at 39.6 and 14.5 eV, respectively. Positive and negative contrasts are given by the black and white regions of the image, and regions of zero contrast are gray. Outlines [red (darker) for monolayer graphene, green (lighter) for bilayer] are drawn to help the comparison.

ing (e.g., *AB* plus *AC*) could appear to be six-fold symmetric. Second, graphene may not be Bernal stacked above the buffer layer. For example, it would be six-fold symmetric if the carbon atoms of the first graphene monolayer were positioned directly above the carbon atoms of the buffer layer (*AA* stacking).

On the contrary, within each two- and three-layer region in panel 3(d), the asymmetry contrast image reveals regions of black and white contrast suggesting the presence of three-fold symmetry in these regions. Bilayer films that are nearly *AA* stacked, such as proposed in Ref. 25, are not apparent here since they would possess a six-fold diffraction pattern and appear gray in panel (d). They would also be distinguishable from monolayer graphene by the presence of two minima in the bright-field reflectivity.[21,22] The black and white regions observed in panel (d) correspond to stacking domains with sizes on the order of 100 nm for our samples, and are smaller than the domains of uniform thickness seen in the bright-field images [Figs. 3(a) and 3(b)]. Where the stacking domains impinge, a linear defect (domain boundary) occurs as in panel (e). Since the boundary between a black and white region in panel (d) corresponds to a disruption in one or more of the graphene planes, these domains likely play an important role in the transport properties of bilayer and multilayer graphene films. Thus, the dark-field imaging reveals that stacking domains and their associated domain boundaries occur within regions of otherwise uniformly thick graphene. These defects are in addition to those defects that result from changes in graphene thickness, and illustrate the complexity that can occur in graphene synthesized from thermally decomposing SiC. Our finding of three-fold domains in bilayer graphene agree with the recent results of Hibino *et al.*[26]

Figure 4 shows the diffraction asymmetry from the 6$\times$6 satellite spots, which result from electrons that interact with the SiC lattice and overlayers through multiple diffraction.[27] These satellite spots also possess three-fold symmetry (a summary of diffraction symmetries is given in Table I). In the asymmetry contrast image of panel (c), the buffer layer has shades of light and dark gray, and the single-layer graphene has regions of black and white. Comparing panel 4(c) to Fig. 2(d) (the same region of the sample), the regions of asymmetry in the buffer layer are the same for both the satellite spots and the SiC spots. LEED from one-layer graphene on a single Ru(0001) terrace[28] is also three-fold symmetric, as are some patterns from graphene on SiC,[29] likely because the substrate terraces were of similar size to the micro-LEED beamspot.

Superstructure in the graphene overlayers could also contribute to Figs. 4(c) and 4(d). For example, the rippling of the thin graphene overlayers has been indicated theoretically[10] and experimentally,[14] and is believed to be responsible for variations in the size of the monolayer graphene band gap.[30]

In conclusion, we have studied the crystallographic structure of epitaxial graphene. We find that there is a fundamental difference in the stacking of the buffer layer, monolayer and bilayer graphene on top of the SiC substrate. We show that the structure of the buffer layer is more complex than previously expected, and that dark-field LEEM provides a method to directly characterize the domain sizes of bilayer graphene and to extract information about the structure of the SiC interface beneath few-monolayer graphene films. We anticipate that the ability to image these crystal symmetries will

continue to enhance our understanding of the properties of thin graphene films on various substrates in the future.

We thank D.-H. Lee for useful discussions. LEEM measurements and sample growth were supported by the Division of Materials Sciences and Engineering of the U.S. Department of Energy under Contracts No. DEAC03-76SF00098 (LBL) and DE-AC04-94AL85000 (SNL). Sample growth was also supported by the MRSEC project through the National Science Foundation.

*Author to whom correspondence should be addressed; alanzara@lbl.gov

[1] A. E. Karu and M. Beer, J. Appl. Phys. **37**, 2179 (1966).
[2] P. W. Sutter, J.-I. Flege, and E. A. Sutter, Nature Mater. **7**, 406 (2008).
[3] C. Berger, Z. Song, T. Li, X. Li, A. Y. Ogbazghi, R. Feng, Z. Dai, A. N. Marchenkov, E. H. Conrad, P. N. First, and W. A. de Heer, J. Phys. Chem. B **108**, 19912 (2004).
[4] C. A. F. Vaz, J. A. C. Bland, and G. Lauhoff, Rep. Prog. Phys. **71**, 056501 (2008).
[5] T. Kawasaki, T. Ichimura, H. Kishimoto, A. A. Akber, T. Ogawa, and C. Oshima, Surf. Rev. Lett. **9**, 1459 (2002).
[6] G. Giovannetti, P. A. Khomyakov, G. Brocks, P. J. Kelly, and J. van den Brink, Phys. Rev. B **76**, 073103 (2007).
[7] T. Ohta, A. Bostwick, T. Seyller, K. Horn, and E. Rotenberg, Science **313**, 951 (2006).
[8] X. Blase, A. Rubio, S. G. Louie, and M. L. Cohen, Phys. Rev. B **51**, 6868 (1995).
[9] S. Y. Zhou, G.-H. Gweon, A. V. Fedorov, P. N. First, W. A. de Heer, D.-H. Lee, F. Guinea, A. H. Castro Neto, and A. Lanzara, NatureMater. **6**, 770 (2007).
[10] S. Kim, J. Ihm, H. J. Choi, and Y.-W. Son, Phys. Rev. Lett. **100**, 176802 (2008).
[11] J. Hass, W. A. de Heer, and E. H. Conrad, J. Phys.: Condens. Matter **20**, 323202 (2008).
[12] F. Varchon, R. Feng, J. Hass, X. Li, B. N. Nguyen, C. Naud, P. Mallet, J.-Y. Veuillen, C. Berger, E. H. Conrad, and L. Magaud, Phys. Rev. Lett. **99**, 126805 (2007).
[13] M. Sprinkle, D. Siegel, Y. Hu, J. Hicks, P. Soukiassian, A. Tejeda, A. Taleb-Ibrahimi, P. Le Fèvre, F. Bertran, C. Berger, W. de Heer, A. Lanzara, and E. Conrad, arXiv:0907.5222 (unpublished).
[14] F. Varchon, P. Mallet, J.-Y. Veuillen, and L. Magaud, Phys. Rev. B **77**, 235412 (2008).
[15] I. Brihuega, P. Mallet, C. Bena, S. Bose, C. Michaelis, L. Vitali, F. Varchon, L. Magaud, K. Kern, and J. Veuillen, Phys. Rev. Lett. **101**, 206802 (2008).
[16] D. Tománek, S. G. Louie, H. J. Mamin, D. W. Abraham, R. E. Thomson, E. Ganz, and J. Clarke, Phys. Rev. B **35**, 7790 (1987).
[17] J. de la Figuera, N. C. Bartelt, and K. F. McCarty, Surf. Sci. **600**, L105 (2006).
[18] E. Rollings, G.-H. Gweon, S. Y. Zhou, B. S. Mun, J. L. McChesney, B. S. Hussain, A. V. Fedorov, P. N. First, W. A. de Heer, and A. Lanzara, J. Phys. Chem. Solids **67**, 2172 (2006).
[19] A. Mattausch and O. Pankratov, Phys. Rev. Lett. **99**, 076802 (2007).
[20] K. V. Emtsev, F. Speck, Th. Seyller, L. Ley, and J. D. Riley, Phys. Rev. B **77**, 155303 (2008).
[21] T. Ohta, F. El Gabaly, A. Bostwick, J. L. McChesney, K. V. Emtsev, A. K. Schmid, T. Seyller, K. Horn, and E. Rotenberg, New J. Phys. **10**, 023034 (2008).
[22] H. Hibino, H. Kageshima, F. Maeda, M. Nagase, Y. Kobayashi, and H. Yamaguchi, Phys. Rev. B **77**, 075413 (2008).
[23] D. A. Siegel, S. Y. Zhou, F. El Gabaly, A. V. Fedorov, A. K. Schmid, and A. Lanzara, Appl. Phys. Lett. **93**, 243119 (2008).
[24] I. Forbeaux, J.-M. Themlin, and J.-M. Debever, Phys. Rev. B **58**, 16396 (1998).
[25] P. Lauffer, K. V. Emtsev, R. Graupner, Th. Seyller, L. Ley, S. A. Reshanov, and H. B. Weber, Phys. Rev. B **77**, 155426 (2008).
[26] H. Hibino, S. Mizuno, H. Kageshima, M. Nagase, and H. Yamaguchi, Phys. Rev. B **80**, 085406 (2009).
[27] Hu Zi-Pu, D. F. Ogletree, M. A. van Hove, and G. A. Somorjai, Surf. Sci. **180**, 433 (1987).
[28] K. F. McCarty, P. J. Feibelman, E. Loginova, and N. C. Bartelt, Carbon **47**, 1806 (2009).
[29] C. Virojanadara, M. Syvajarvi, R. Yakimova, L. I. Johansson, A. A. Zakharov, and T. Balasubramanian, Phys. Rev. B **78**, 245403 (2008).
[30] L. Vitali, C. Riedl, R. Ohmann, I. Brihuega, U. Starke, and K. Kern, Surf. Sci. **602**, L127 (2008).